Micron 43 (2012) 961–970

Contents lists available at SciVerse ScienceDirect

Micron

journal homepage: www.elsevier.com/locate/micron

Morphometric partitioning of the respiratory surface area and diffusion capacity of the gills and swim bladder in juvenile Amazonian air-breathing fish, *Arapaima gigas*

Marisa Narciso Fernandes [a,*], André Luis da Cruz [b], Oscar Tadeu Ferreira da Costa [c], Steven Franklin Perry [d]

[a] *Department of Physiological Sciences, Federal University of São Carlos, Rod. Washington Luis km 235, 13565-905 São Carlos, SP, Brazil*
[b] *Department of Zoology, Institute of Biology, Federal University of Bahia, Rua Barão de Geremoabo 147 – Campus de Ondina, 40170-970 Salvador, BA, Brazil*
[c] *Department of Morphology, Federal University of Amazonas, Avenida General Rodrigo Octávio Jordão Ramos, 3000, 69077-000 Manaus, AM, Brazil*
[d] *Institute of Zoology, Bonn University, Poppelsdorfer Schloss, 53115 Bonn, Germany*

ARTICLE INFO

Article history:
Received 14 December 2011
Received in revised form 16 March 2012
Accepted 23 March 2012

Key words:
Bimodal respiration
Lamellar surface area
Water/air–blood barrier thickness
Stereology
Teleost

ABSTRACT

The gills and the respiratory swim bladders of juvenile specimens (mean body mass 100 g) of the basal teleost *Arapaima gigas* (Cuvier 1829) were evaluated using stereological methods in vertical sections. The surface areas, harmonic mean barrier thicknesses and morphometric diffusing capacities for oxygen and carbon dioxide were estimated. The average respiratory surface area of the swim bladder (2173 $cm^2\ kg^{-1}$) exceeded that of the gills (780 $cm^2\ kg^{-1}$) by a factor of 2.79. Due to the extremely thin air–blood barrier in the swim bladder (harmonic mean 0.22 μm) and the much thicker water–blood barrier of the gills (9.61 μm), the morphometric diffusing capacity for oxygen and carbon dioxide was 88 times greater in the swim bladder than in the gills. These data clearly indicate the importance of the swim bladder, even in juvenile *A. gigas* that still engage in aquatic respiration. Because of the much greater diffusion constant of CO_2 than O_2 in water, the gills also remain important for CO_2 release.

1. Introduction

Bimodal breathing (i.e., oxygen uptake from the water by gills and from the air by an air-breathing organ) has evolved many times among teleost fishes. Within bimodal breathers, amphibious species, which can breathe in or out of water, can be distinguished from aquatic species, which surface to breathe air while remaining in the water (Graham, 1997). In addition, obligate air breathers, who are dependent on aerial gas exchange, can be differentiated from facultative air breathers, who only supplement their oxygen needs by air breathing (Hughes et al., 1974; Fernandes, 1996; Perna and Fernandes, 1996; Santos et al., 1994; Mazon et al., 1998; Moraes et al., 2005; Fernandes et al., 2007; Cruz et al., 2009b). The accessory air-breathing organs are located in the region of the head consisting of buccal and pharynx epithelia, pharynx pouches, modified branchial and opercular surfaces (Munshi, 1985), structures localized in the digestive tract (stomach and intestinal tract) (Carter and Beadle, 1931; Gee and Graham, 1978; Silva et al., 1997; Cruz et al., 2009a) and skin (Banerjee and Mittal, 1976; Bicudo and Johansen, 1979; Moraes et al., 2005).

The basal teleost *Arapaima gigas* (Cuvier 1829; Osteoglossidae), commonly referred to as the "pirarucu", is an aquatic obligate air-breather that uses its swim bladder to breathe atmospheric air. Its gills exhibit pronounced changes as the fish matures. Small fish have gill filaments with well-defined lamellae (Brauner et al., 2004; Costa et al., 2007), while large fish have column-shaped filaments that appear to have a smooth surface (Brauner et al., 2004) but still have atrophied lamellae (Ramos, 2008). *A. gigas* inhabits oxygen-poor water in lakes and flooded forest in the Amazon basin and is one of largest freshwater fish species in the world, growing anywhere from 7 to 10 kg in the first year (Pereira-Filho et al., 2003).

The *A. gigas* swim bladder is highly vascularized and adapted for aerial respiration (Graham, 1997). Early studies reported that in 1- to 3-kg fish, between 75% and 95% of the total oxygen uptake was derived from the air (Sawaya, 1946; Stevens and Holeton, 1978). Brauner and Val (1996) confirmed these values for 1.7-kg fish, showing that 79% of their total excreted CO_2 was processed through the gills. Juvenile (10–100 g) *A. gigas* are less dependent on aerial respiration than the adults are (Brauner et al., 2004; Brauner and Val, 2005). Recently, O_2 uptake and CO_2 excretion measurements in small (67 g) and large (724 g) *A. gigas* showed that the specific O_2 uptake rate ($\mu molO_2\ g^{-1}\ h^{-1}$) of small pirarucu is

* Corresponding author at: Department of Physiological Sciences, Federal University of São Carlos, Rod. Washington Luis km 235, 13565-905 São Carlos, SP, Brazil. Tel.: +55 16 3351 8742; fax: +55 16 3351 8401.
E-mail address: dmnf@ufscar.br (M.N. Fernandes).

0968-4328/$ – see front matter © 2012 Elsevier Ltd. All rights reserved.
http://dx.doi.org/10.1016/j.micron.2012.03.018

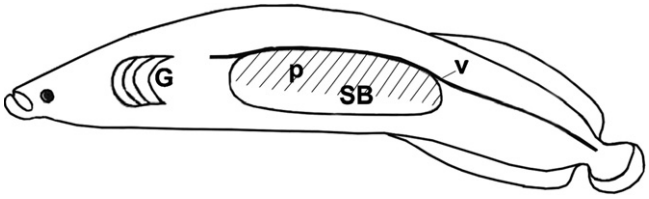

Fig. 1. Diagram illustrating the position of gills (G) and swim bladder (SB) of *A. gigas*. The parenchyma (p) position in the swim bladder was also indicated. v, vertebra.
Source: Modified from Val and Almeida-Val (1995).

two-thirds that of the large ones, and the water fraction of O_2 uptake and CO_2 excretion is lower in small individuals, despite the drastic morphological changes in the gills as the fish matures (Gonzalez et al., 2010).

Physiological studies have documented the bimodal gas exchange in *A. gigas* (Brauner and Val, 1996; Brauner et al., 2004; Gonzalez et al., 2010). However, morphological data on respiratory organs are scarce. Recently, the gill surface area of small *A. gigas* was estimated to be similar to sluggish water-breathing and facultative air-breathing fish (Costa et al., 2007), but no data on swim bladder surface area are currently available. The present study delivers morphometrical data for the gas exchange organs of fish at a critical stage in their development where they are obligate air breathers but still engage in aquatic respiration. The main goal of the present study was to quantify the relative morphological adaptation of gill and swim bladder partitioning for gas exchange in juvenile *A. gigas*. To this end, the surface area, diffusion barrier thickness and the morphometric diffusion capacity for O_2 and CO_2 of the gills and the swim bladder were estimated using the same stereological methods in vertical sections, thus ensuring a comparison that is free of methodological differences.

2. Materials and methods

This study was conducted in accordance with national and institutional guidelines for the protection of human and animal welfare. Six juvenile *A. gigas* [body mass (M_B) = 85–110 g; mean = 100 ± 9 g; body length (L_B) = 20–26 cm; mean = 24 ± 2 cm] were obtained from a commercial fish culture in Ribeirão Preto, SP, Brazil, and were maintained in tanks at the Federal University of São Carlos (SP) at 25 °C. Lightly anesthetized (0.5% Benzocaine®, Sigma) fish were killed by a blow to the head. The gills were immediately removed and fixed by immersion in 2.5% phosphate-buffered glutaraldehyde solution with a pH of 7.8 and an osmolality of approximately 300 mOsmol. The specimen was then opened ventrally, and the swim bladder was exposed and filled with fixative solution. Next, the entire fish was immersed in the abovementioned fixative at 4 °C. Fig. 1 shows a diagram indicating the gills and swim bladder position.

2.1. Sampling and processing for light (LM) and transmission electron (TEM) microscopy

The sampling and embedding procedures were designed to combine the Cavalieri principle for determining the reference volume with the stereological vertical sectioning method for measuring surface area, as described by Moraes et al. (2005) for the swim bladder and by Costa et al. (2007) for gills.

2.1.1. Gills

The gill arches from each fish (left and right side) were separated and processed for stereological estimation of surface area and barrier thickness of gills in vertical sections as described by Costa et al. (2007). Briefly, the rakers and bone of the epibranchial and ceratobranchial elements of each gill arch were removed in the way that the gill filaments from anterior and posterior hemibranchs were kept attached in the gill arch tissue. The epi- and ceratobranchial portions were separated, and the latter portion was cut in half yielding three samples from each gill arch (Fig. 2A and B). The samples were dehydrated by graded ethanol series and embedded in Historesin®. Random numbers were assigned to the samples, and then, the samples were placed with the opercular side (horizontal plane) down. The vertical axis was perpendicular to the horizontal plane. The samples were embedded in methacrylate in stacks of 3, one atop the other, with each sample rotated sequentially +15° relative to the previous one around the vertical axis. Historesin® (Leica, Heidelberg, Germany) was used as the embedding methacrylate due to the negligible shrinkage of section and the fish tissue (Cruz et al., 2009b). The entire gill from one side of the animal was contained in four blocks, properly oriented for stereological vertical sectioning. Ten equidistantly spaced vertical sections of a 3-μm thickness that had been stained with toluidine blue and acid fuchsin were used to estimate the gill volume using the Cavalieri method as well as the surface area in vertical uniform random (VUR) sections (Michel and Cruz-Orive, 1988).

Surface area and volume of the gills were determined using stereological point and intersection counting methods (Howard and Reed, 2007; Costa et al., 2007) under a BX51 Olympus microscope with a 20×/0.80 oil immersion lens (Fig. 2C and E). The images were captured by a JVC-TKC1380 digital video camera and were analyzed at a final magnification of 759× with the CAST System software, version 2.00 (Olympus Denmark S/A).

The water–blood diffusion distance was estimated using the same sections at 3807× magnification and a 100×/1.40 oil immersion objective lens (Fig. 2D). Distances were measured along sine-weighted lines generated on the VUR sections of gills, as described by Gundersen et al. (1988). A new angle was selected at random for each histological section. The harmonic mean thickness of the air–blood barrier was then measured as 2/3 the harmonic mean intercept length (Weibel and Knight, 1964).

2.1.2. Swim bladder

The fixed swim bladder was removed and transected by 10 equidistantly spaced slices, beginning at a random starting point within the first interval (Moraes et al., 2005). A square lattice grid was placed on the anterior surface of each section and point counts of the projected surfaces of the parenchyma, central lumen and ventral membrane were performed (Fig. 3A and B). The volume of these three components was estimated using the Cavalieri method (Michel and Cruz-Orive, 1988), and 10 tissue samples from the parenchyma of each fish were then taken by systematic random sampling and processed for light microcopy to estimate the differential tissue volume. The samples were rotated +18° relative to the previous one and embedded in Historesin® (Leica) with the adventitial side down, defining the horizontal plane. Tissue was sectioned vertically (3 μm thickness) and stained with toluidine blue and acid fuchsin. To measure differential tissue volumes and the respiratory surface area, stereological point and intersection counting methods (Fig. 3C and D) were employed using the CAST System software.

To measure the air–blood distance, 10 systematic random samples were taken from the posterior surface of swim bladder slices of each fish and processed for transmission electron microscopy. The samples were embedded in Epon 812® (EMS, Hatfield, EUA) sectioned at 60 nm in thickness and contrasted on 300 mesh grids using standard uranyl acetate and lead citrate procedures. For each animal, 10 electron micrographs of randomly chosen fields showing the potential respiratory surface were taken at approximately 3000× and 12,000× using a Zeiss EM 10 electron microscope. The exact magnification was calculated for each series of electron micrographs with the aid of a calibration grid. A modified

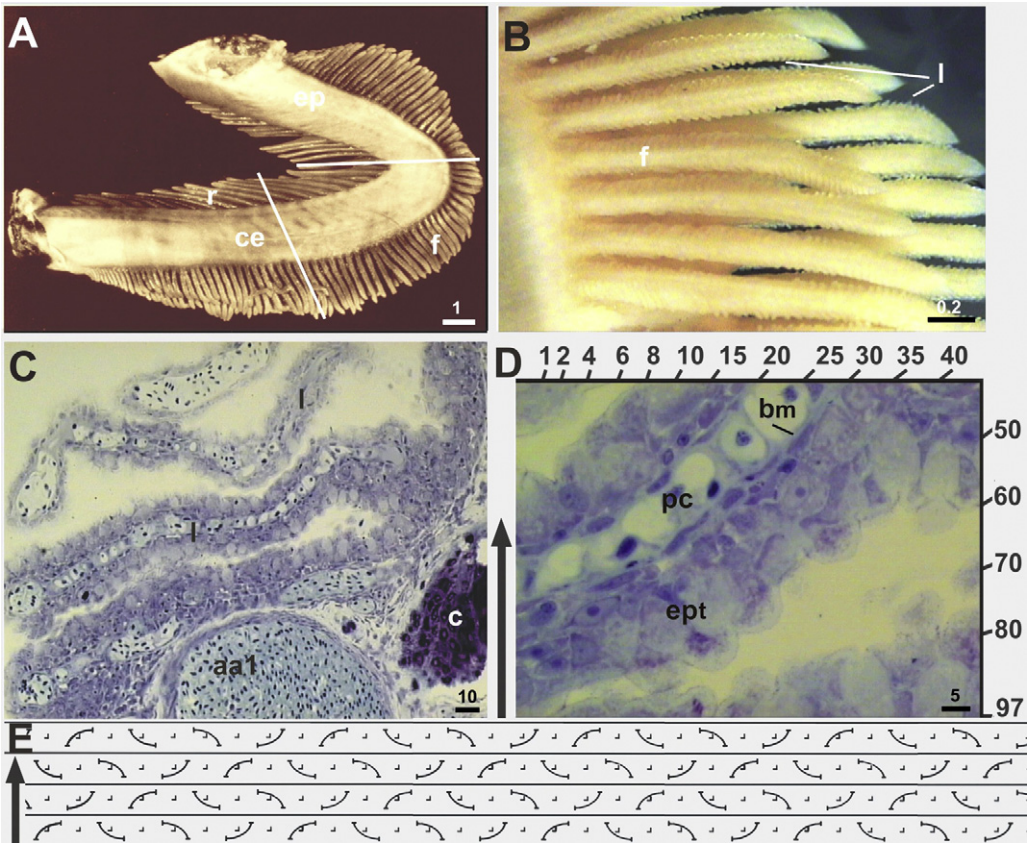

Fig. 2. *A. gigas* gills. (A) Representative gill arch (1st gill arch) showing rakers (r), filaments (f), epibranchial bone (ep) and ceratobranchial bone (ce). White lines indicate the gill arch sectioning for embedding. Scale bar is in mm. (B) Filament (f) showing the lamellae (l) on both sides of the filament long axis. Scale bar is in mm. (C) Light micrograph illustrating a vertical section of gill filament. Primary afferent artery (aa1), cartilage ray (c), lamella (l). Scale bar is in μm. (D) High magnification of a gill filament vertical section showing a lamella and a sine-weighted orientation frame. Direction of blood–water barrier measurements is assigned randomly between 1 and 97. Basement membrane (bm), epithelium (ept), pillar cell (pc). Scale bar is in μm. (E) Portion of the test array that was superimposed on the microscopic image (C) for the estimation of the Cavalieri volume and surface-area-to-volume ratio. The arrow indicates the vertical axis of gill sections and test array.

Merz test array (Perry, 1978) and standard point and intersection counting methods (Howard and Reed, 2007) were used to determine the dimensions of the air–blood barrier elements (Fig. 4A). The intersections were used as starting points to estimate the air–blood diffusion distance (Fig. 4A). The harmonic mean thickness of the air–blood barrier was measured as 2/3 the harmonic mean intercept length (Weibel and Knight, 1964) directly on the systematically rotated TEM negatives using a dissecting microscope equipped with a drawing tube to superposition the stereological test array (Perry et al., 1994).

2.2. Anatomical diffusion factor and the morphometric diffusion capacity of the water–blood or air–blood barrier

The anatomical diffusion factor (ADF) of the tissue barrier of the gills and swim bladder was estimated directly from the stereological data as the quotient of the respiratory surface area in relation to body mass (S_R/M_B) and the harmonic mean of the diffusion barrier thickness (τ_h) of the respective organ (Perry et al., 1994). The morphometric diffusion capacity (D*m*) was calculated as the product of the ADF and the weighted mean (see below) of Krogh's diffusion coefficient (*K*) for the respective cell layers (epithelium/endothelium/pillar cells) or basal membrane/connective tissue (for gills and swim bladder) of the diffusion barrier. The volume proportion of the different components was estimated separately by point counting (Fig. 3B). Each gill or swim bladder element was multiplied by the appropriate *K* value (see below), and this weighted numerical ratio yielded a *K* value for oxygen (K_{O_2}) or CO_2 (K_{CO_2}) in the water (air)–blood barrier corrected to 25 °C. Because the physical constants for fish tissue are lacking, the calculations were performed using the constants for rat lung tissue to represent epithelium, endothelium and pillar cells, and frog connective tissue to represent connective tissue and basal membrane (Bartels, 1971).

2.3. Statistical analyses

Descriptive statistics were performed using standard spreadsheet software (Microsoft Excel®). The relative and absolute variables were first calculated for each animal in accordance with Gundersen and Jensen (1987) and Howard and Reed (2007) to determine the precision of the estimates of volume, area and barrier thickness measurements. To evaluate the variability between animals, the mean values were accompanied by the respective standards errors (SEM) for the gills and swim bladder in accordance with Howard and Reed (2007). Because the standard deviation of a harmonic mean has not been defined, the range of harmonic means is provided, as well.

3. Results

3.1. General structure of gills and swim bladder

The gills of *A. gigas* had the same basic structure as those seen in most teleost fish: four gill arches, each bearing two rows of filaments (Fig. 2A and B). Lamellae, the gas-exchange units of the gills,

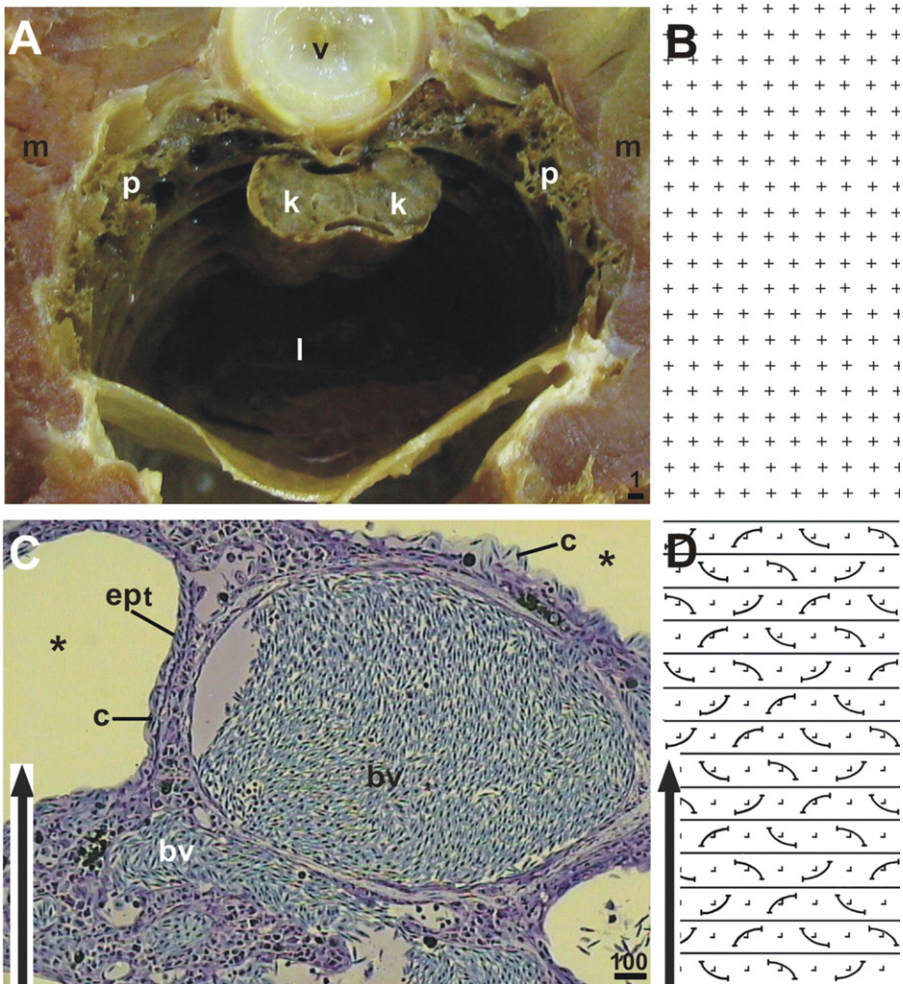

Fig. 3. *A. gigas* swim bladder. (A) Cross section of swim bladder showing the parenchyma (p) in the dorso-lateral region of the swim bladder and the lumen (l). Kidney (k), muscles (m), vertebra (v). Scale bar is in mm. (B) Portion of the test array that was superimposed on the swim bladder cross section for the evaluation of the Cavalieri volume. (C) Light micrograph illustrating a vertical section of swim bladder parenchyma showing edicular spaces (*), blood vessels (bv), capillaries (c) and parenchyma epithelium (ept). Scale bar is in μm. (D) Portion of the test array that was superimposed on the microscopic image to estimate the differential swim bladder tissue volume and surface-area-to-volume ratio. The arrows indicate the vertical axis of gill section and test array.

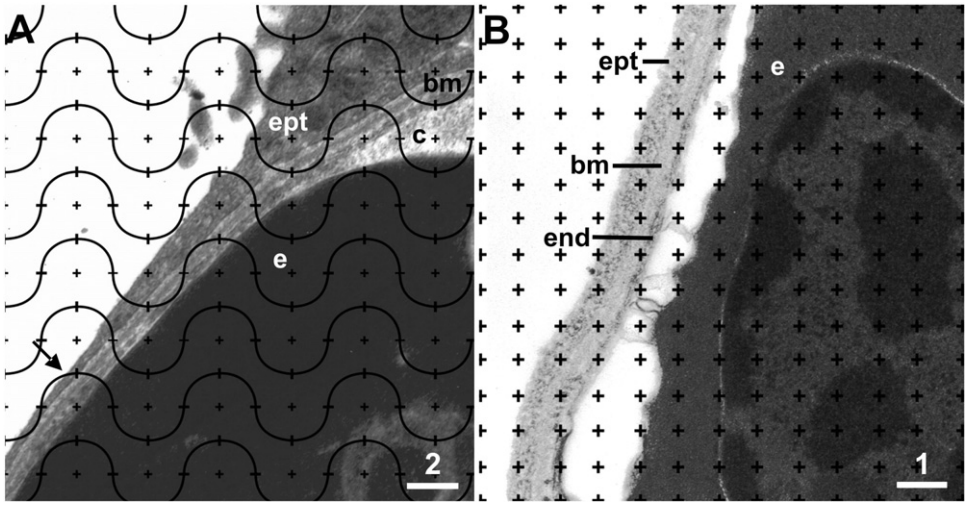

Fig. 4. (A) Modified Merz grid superimposed on the TEM micrograph. Intersection points (arrows) indicate starting points for randomly oriented measurements of blood–air barrier. Basal lamina (bl), capillary (c), epithelium (ept). Scale bar is in μm. (B) Square lattice graticule to perform point counting for estimation of volume proportion of blood–air barrier components superimposed on TEM micrograph. Epithelium (ept), basal lamina (bl) and endothelium (end). Scale bar is in μm.

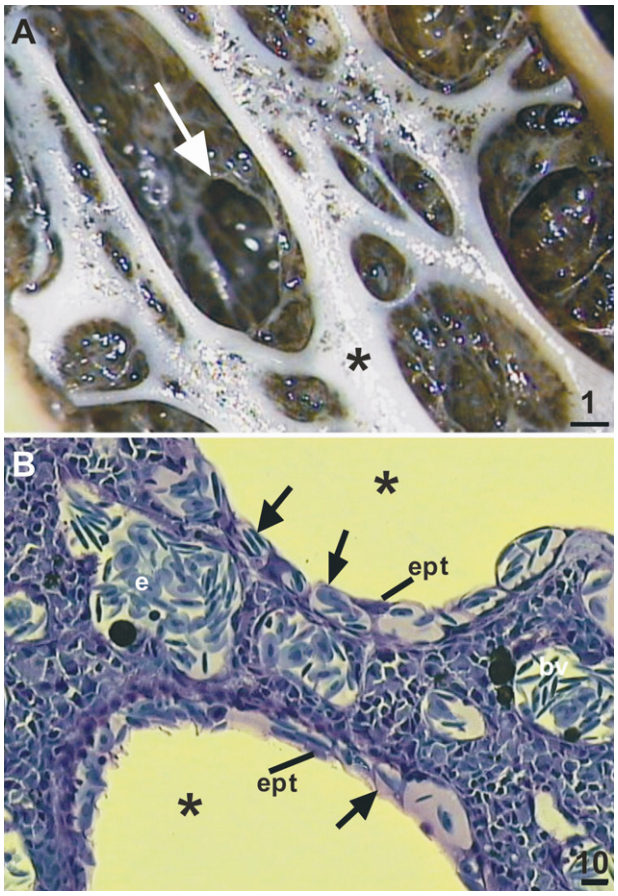

Fig. 5. *A. gigas* swim bladder. (A) Respiratory region (parenchyma) of the swim bladder viewed from the lumen, showing trabeculae (*) and edicular spaces containing respiratory septa (arrow). Scale bar is in μm. (B) Respiratory tissue of an interradicular septum, showing capillaries (arrow) underlying the epithelium (ept). Large blood vessel (bv); erythrocyte (e); (*) edicular air space. Scale bar is in μm.

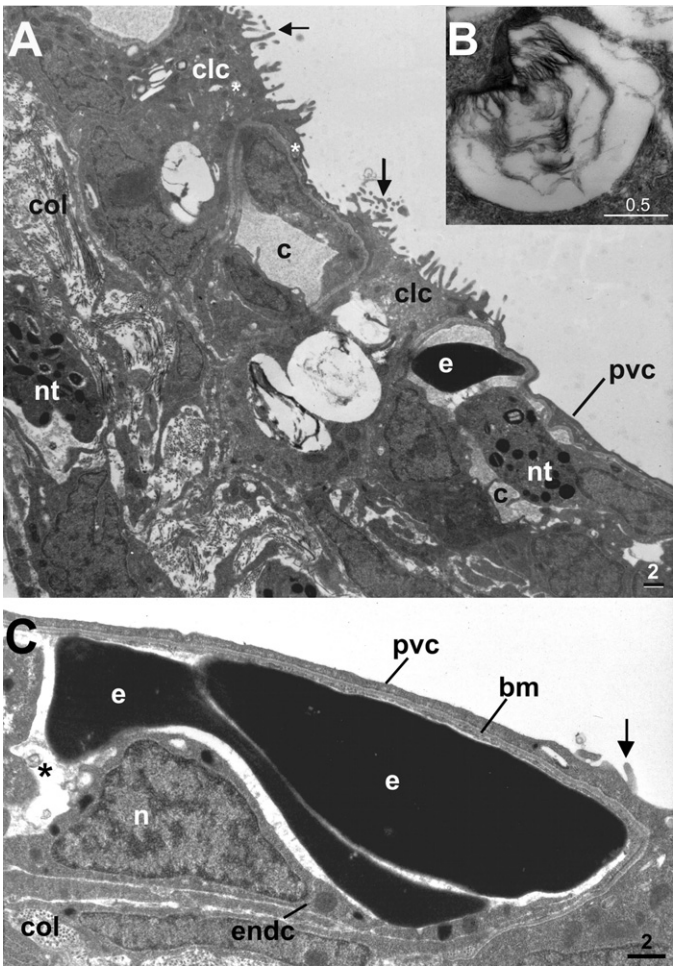

Fig. 6. *A. gigas* swim bladder. (A) TEM swim bladder parenchyma showing pavement (pvc) and columnar (clc) cells in the respiratory epithelium and the capillaries (c) under the basal lamina. Note the high density of collagen fibers (col) and blood vessels (bv) on the inner parenchyma. Arrows indicate microvilli on the epithelial cell surface and (*) lamellar bodies. Erythrocyte (e); neutrophils (nt). Scale bar is in μm. (B) High magnification of a lamellar body. Scale bar is in μm. (C) High magnification of the air–blood barrier showing smooth surface pavement cells (pvc), basal lamina (bl) and endothelial cells (endc) of the capillary (*). Erythrocyte (e); collagen (col); nucleus (n). Scale bar is in μm.

projected from both sides of the filaments (Fig. 2B). The lamellae consisted of the pillar cell system covered by basement membrane and two or three epithelial cell layers (Fig. 2C). In general, the cells of the innermost epithelial cell layer were flat and those of the outermost cell layer were cuboidal (Fig. 2C and D). Mucous and chloride cells were distributed throughout the filament epithelium, which was stratified and contained in 5–7 cell layers.

The swim bladder lay ventral to the vertebral column and was fused to dorsal muscles of the body wall and ribs (Figs. 1 and 3A, B). It extended the full length of the body cavity from the posterior part of the head and kidneys to the posterior end of the intestine. The trunk kidneys projected dorsally as a median ridge into the lumen of the swim bladder (Fig. 3B). The highly vascularized, dorsolateral wall of *Arapaima*'s swim bladder constituted the parenchymal layer (Fig. 3B and C) that also enveloped the kidneys. The parenchyma was contiguous with a tough, translucent membrane that delimited the central lumen of the organ ventrally (Fig. 3A and B). This membrane contained some capillaries close to the mucosal surface, and their potential respiratory function could not be completely disregarded. The parenchyma was irregularly subdivided by numerous septa to form compartments (ediculae) of highly variable size (Fig. 5A) that were supported by smooth muscular trabeculae, which consisted of a connective tissue matrix with numerous large and small blood vessels.

The parenchyma tissue consisted of numerous small vessels and a dense capillary layer just below the respiratory epithelium (Fig. 5B). The respiratory epithelium covered all surfaces of the ediculae and consisted of pavement and columnar epithelial cells. The pavement cells had a low number of mitochondria, very small lamellar bodies and, in general, were underlined by the capillaries and separated from them by the basal lamina (Figs. 4B and 6C). The apical surface of pavement cells was smooth with short microvilli distributed at the cell border (Figs. 4A and 6A). Columnar cells were distributed among the pavement cells. They were characterized by microvilli at the cell surface and numerous mitochondria and lamellar bodies of different sizes (Fig. 6A). The lamellar bodies reached up to 1.5 μm in diameter (Fig. 6B). Tight junctions characterized the junction complex between pavement and columnar cells. Numerous neutrophils were found in the capillaries and blood vessels. The parenchyma tissue was rich in collagen fibers consisting of a layer between the capillaries and the small and large blood vessels in the inner tissue (Fig. 6A). The air–blood barrier (Fig. 6C) was composed of the endothelial cells of capillaries (23%), basal lamina of the swim bladder epithelium (24%) and the pavement epithelial cells themselves (57%).

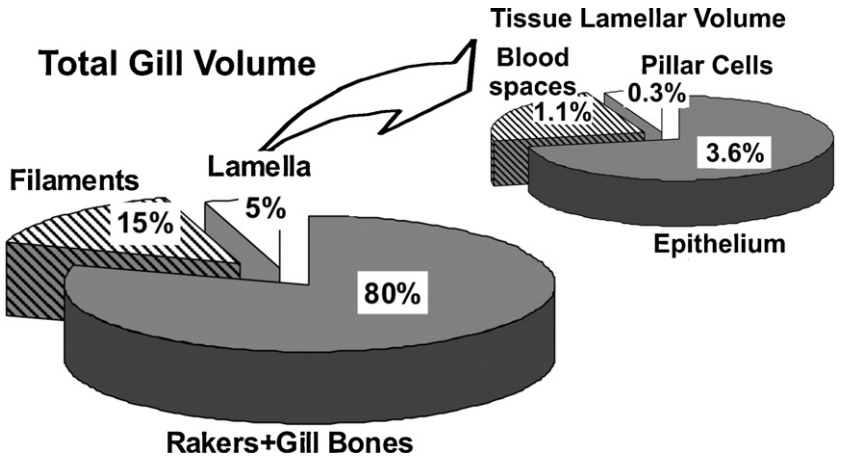

Fig. 7. *A. gigas* gills. Percentage volumes of the gill structural elements including rakers, gill arch bones, filaments and lamellae. The arrow indicates the volume percentages of the elements of the lamellae.

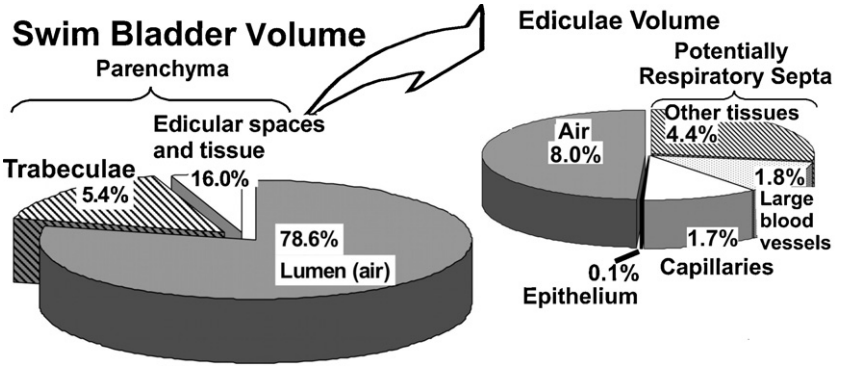

Fig. 8. *A. gigas* swim bladder. Volume percentages of elements in the entire swim bladder. *Note*: trabeculae are non-respiratory elements. The arrow indicates the volume percentages of elements of parenchyma, excluding the (non-respiratory) trabeculae.

3.2. Morphometry of gills and swim bladder

3.2.1. Structural parameters

The gills of juvenile *A. gigas* had a volume of $7.5 \pm 0.3\ cm^3$ including rakers, epi- and ceratobranchial bones, filaments and lamella. Most of total gill volume (80%) consisted of the long rakers and branchial bones. The gill filaments made up only 15% of the total gill volume, while 5% was ascribed to the lamellae (3.6% epithelium, 1.1% blood spaces and 0.3% pillar cells; Fig. 7).

The swim bladder length was approximately 0.7 of the total body length with a total volume of $9.5 \pm 0.3\ cm^3$. Most of this volume ($7.5\ cm^3$) represented the air in the central lumen and correspond to 78.6% of total swim bladder volume) (Fig. 8). The volume of ventral membrane and the parenchyma of swim bladder was $0.5\ cm^3$ and $1.6\ cm^3$ which corresponded to 5.4% and 16% of the total swim bladder volume, respectively (Fig. 8). The tissue of the respiratory portion of the swim bladder (parenchyma excluding the trabeculae and trabecula air) consisted of 0.1% epithelium, 1.7% capillaries and 1.8% large vessels and approximately 4.4% of other tissues, such as connective tissue and nerves (Fig. 7).

3.2.2. Gas-exchange parameters

The mean respiratory surface area of the protruded lamella (portion of the lamellae that contacts water) was $780.21 \pm 31.23\ cm^2\ kg^{-1}$ (Table 1), ranging from 690.06 to $880.96\ cm^2\ kg^{-1}$. This represented approximately 70% of filament and lamellar surface areas taken together. The potential respiratory surface area of the lamellae was 5.1 times greater than the filament surface area.

The surface area of the ediculae tissue of swim bladder was $2173.05 \pm 118.89\ cm^2\ kg^{-1}$ (Table 1). Of this area, $1912.39\ cm^2\ kg^{-1}$ (94%) was potentially respiratory, while $167.97\ cm^2\ kg^{-1}$ (6%) was not potentially respiratory. The latter consisted of large trabeculae that lacked capillaries under the epithelium. Thus, the potentially respiratory surface area of parenchyma of swim bladder was 2.8 times greater than that of gill lamellae in these juvenile specimens.

The gill lamellar epithelium had an arithmetic mean thickness of $18.15 \pm 1.34\ \mu m$ and ranged from 14.76 to 22.72 μm. The harmonic mean was 9.61 (range, 8.1–12.2 μm) (Table 1). The gas-exchange barrier of the swim bladder had an arithmetic mean of $1.56 \pm 0.44\ \mu m$ with a range of 1.08–2.71 μm, and its harmonic mean was 0.22 μm, ranging from 0.16 to 0.43 μm (Table 1). In the large trabeculae regions the harmonic mean is up to 5–7 μm higher as there is not capillaries just under the

Table 1
Dimensions (means ± SEM) of the respiratory organs of the pirarucu, *Arapaima gigas* ($M_B = 100 \pm 9$ g).

Parameter	Gills	Swim bladder
Total respiratory surface area (cm^2)	76.36 ± 2.27	157.01
Respiratory surface area ($cm^2\ kg^{-1}$)	780.21 ± 31.23	2173.05 ± 118.89
Arithmetic mean of water/blood or air/blood barrier (μm)	18.15 ± 1.34	1.56 ± 0.44
Harmonic mean of water/blood or air/blood barrier (μm)	9.61 Range 8.10–12.16	0.22 Range 0.16–0.43
ADF ($cm^2\ \mu m^{-1}\ kg^{-1}$)	80.62 ± 5.38	8424.68 ± 752.16
Dm_{O_2} ($cm^3\ min^{-1}\ mmHg^{-1}\ kg^{-1}$)	0.021 ± 0.002	1.86 ± 0.19
Dm_{CO_2} ($cm^3\ min^{-1}\ mmHg^{-1}\ kg^{-1}$)	0.403 ± 0.035	35.545 ± 3.69

epithelium. The anatomical diffusion factor (ADF) of the swim bladder ($8650.74 \pm 752.16\ cm^2\ \mu m^{-1}\ kg^{-1}$) was thus 107.3 times greater than that of the gills ($80.65\ cm^2\ \mu m^{-1}\ kg^{-1}$, Table 1) calculated as the mean of the ADF values for the individual fish.

The morphometric diffusion capacity for O_2 of gills was $0.021 \pm 0.002\ cm^3\ min^{-1}\ mmHg^{-1}\ kg^{-1}$, while that of the swim bladder was 1.86 ± 0.19 ($cm^3\ min^{-1}\ mmHg^{-1}\ kg^{-1}$). The morphometric diffusion capacity for CO_2 was 0.403 ± 0.035 and $35.545 \pm 3.69\ cm^3\ min^{-1}\ mmHg^{-1}\ kg^{-1}$ for the gill lamella and the swim bladder, respectively (Table 1). The morphometric D_{O_2} and D_{CO_2} values of the swim bladder were approximately 88 times greater than those for the gills.

4. Discussion

This study clearly demonstrates the importance of the swim bladder for gas exchange in juvenile *A. gigas*, even at a size where branchial water breathing is still possible. Although the basic gill structure of juvenile *A. gigas* did not differ from that of other species, its respiratory surface area is lower, and its water–blood diffusion barrier is very thick compared to some water-breathing species and similar to those of air-breathing fish (excepting the lungfish which has a non-respiratory functional gills; Table 2). The extensive surface area and the very thin air–blood diffusion barrier of its modified swim bladder shows 2.8 times greater surface area and 43 times thinner gas diffusion distance than in the gills, respectively. Based on these values alone, it is clear whether the swim bladder is the major respiratory organ. Compared to the accessory organs for respiration of other air-breathing fish, the *A. gigas* swim bladder has a larger surface area and a similar air–blood diffusion barrier (Table 2) that favor air respiration.

Physiological data have shown that, in general, three quarters of all O_2 needs are taken up by the swim bladder (Brauner et al., 2004; Gonzalez et al., 2010). Assuming that O_2 is 30 times less soluble than carbon dioxide in water, and assuming that approximately equal molar equivalents of O_2 and CO_2 are taken up and given off, the gills would be able to excrete 30 mol of CO_2 for each mole of O_2 taken up in the swim bladder. Additionally, the diffusion capacity expresses the rate of gas exchange per unit of driving pressure. As the driving pressure for oxygen falls between breaths, the rate of O_2 uptake in the swim bladder will fall accordingly, while it will remain at constant, albeit low, levels in the gills.

Earlier physiological studies suggested that a spatial uncoupling between O_2 uptake in the swim bladder and CO_2 excretion in the gills might occur (Randall et al., 1978; Brauner and Val, 1996). In 2- to 3-kg fish, at least 78% of total O_2 uptake is from air, but only 37% of total CO_2 is excreted into the swim bladder (Randall et al., 1978). Slightly different data were found by Brauner and Val (1996), reporting an O_2 uptake of 78% by the swim bladder with only a 15% CO_2 excretion into this organ. Thus, 79% of CO_2 must have been excreted by the gills with an additional 6% via the kidney in the urine. Recently, Gonzalez et al. (2010) showed that gill morphology changes do not place limitations on O_2 uptake in large fish and that the CO_2 excretion through the gills is similar (85–90%) in small (67 g) and large (724 g) fishes. They also showed that at lower blood pH, P_{CO_2} and concentrations of HCO_3^- in small fish suggest a possible diffusion limitation for CO_2. Ammonia excretion is mainly conducted through the gills. Our morphometric data support this functional partitioning, which may be less pronounced in our juvenile specimens than in large fish.

The respiratory surface area of gills ($78\ cm^2$) of *A. gigas* is smaller than in typical water-breathing fish (see Table 2) and the facultative air breathers such as *Lepisosteus osseus* ($83\ cm^2$; Landolt and Hill, 1975), *Amia calva* ($191\ cm^2$; Crawford, 1971) and *Hoplerythrinus unitaeniatus* ($125\ cm^2$; Fernandes et al., 1994). However, compared with the obligate air breathers such as *Anabas testudineus* ($94\ cm^2$; Hughes et al., 1973) or the American lungfish *Lepidosiren paradoxa* ($0.38\ cm^2$; Moraes et al., 2005), the gill surface areas of small *A. gigas* are relatively well developed (Costa et al., 2007). Low gill surface area in air-breathing fish has been considered an adaptation to reduce the loss of O_2 in hypoxic waters (Graham, 1997). Low surface area and a large water–blood distance reduce the gill diffusion capacity for O_2 uptake, but it may favor the air-breathing fish living in hypoxic and stagnant waters by reducing the O_2 loss into water through the air breathing organ via the gills. It may also solve problems related to osmoregulation by reducing water influx and ion losses. The reversible protrusion of lamellae in the water-breathing fish (*Carassius carassius*) when the O_2 supplying meets the species needs (Sollid et al., 2003; Sollid and Nilsson, 2006) supports the hypothesis that the low gill surface area of *A. gigas* is able to support its ability to live in the hypoxic and ion-poor waters of the rivers of the Amazon basin because the swim bladder is the main respiratory organ in this species. The compromise between gas exchange and other gill functions, such as osmoregulation, acid–base balance and nitrogen excretion, also have to be considered.

The swim bladder of most fish has hydrostatic and some other purposes. Physoclistous swim bladder refers to those in which the pneumatic duct is absent and physostomous swim bladder implies in a presence of a pneumatic duct connecting the organ to the gut through which can be inflated or deflated. In general, both swim bladder types have low blood supply, excepting in air-breathing fish that has a modified swim bladder for atmospheric air respiration. In this case, the swim bladder has a highly vascularized extense trabeculae region which varies among species. In *A. gigas*, the volume percentage of respiratory region of swim bladder in relation to body mass is the smallest among fish that use the swim bladder as both a respiratory organ and a hydrostatic organ (Graham, 1997). The parenchyma occupies only 22% of the swim bladder volume but has a surface-to-volume ratio of $221\ cm^{-1}$, which is greater than that seen in reptilian lungs (Perry, 1983). Just the reverse is seen in the parenchyma of *L. paradoxa* weighing approximately 600 g (Moraes et al., 2005), where the lung volume ($25\ ml\ kg^{-1}$) is too small to achieve neutral buoyancy, but the parenchyma makes up 43% of the total lung volume and has a surface-to-volume ratio of only $129\ cm^{-1}$ (Moraes et al., 2005).

The swim bladder surface area of *A. gigas* is between 5- and 33-fold that of the accessory organs of several air-breathing fish taking oxygen directly from the air (Table 2). Conversely, the thin air–blood barrier of the swim bladder, with a harmonic mean ranging from 0.16 to 0.43 μm, is lower than that of other air-breathing organs (Table 2). It is strikingly similar to that of avian lungs (Maina et al., 1989; Watson et al., 2007;). The air–blood barrier of avian lungs is thinner than that of the rabbit, dog, and horse due to the strikingly thin and uniform interstitial layer of this barrier (West et al., 2006; Watson et al., 2007). As in the avian lung, the parenchymal portion of the *A. gigas* swim bladder is firmly attached to the body wall and is therefore of relatively constant volume. Because the epithelium does not need to be stretched, the epithelial cells can be much thinner. Also, mechanical stability need not be supplied by the connective tissue. In avian, ventilation occurs in a flow-through manner and can be described by a crosscurrent, which potentially has greater efficacy than the concurrent model (alveolar) described for other lungs, although avians has lower vascularized lungs (Powell, 1989). The air-breathing *A. gigas* exhale first and, then inhale the atmospheric air. The air inhalation is the result of the action of a buccal pump combined with the swim bladder aspiration (Farrell and Randall, 1978). The air-breathing mechanism of *A. gigas* is unique among air-breathing fish with a single ventilation of the swim bladder. Aspiration has only been found in some reptiles and birds and mammals, all of whom possess a diaphragm to generate a subatmospheric pressure in the lungs. The ventral membrane of the swim bladder of *A. gigas* may act as a diaphragm-like

Table 2
Morphometric comparison of gill and air-breathing organ (ABO) in several fish species.

Species	Mode of Respiration	Gill		ABO			References
		Area for a 100 g fish (cm^2)	Water/blood barrier thickness, harmonic mean, μ_h (μm)	Area for a 100 g fish (cm^2)		Air/blood barrier thickness, harmonic mean, μ_h (μm)	
Chaenocephalus aceratus	WB	120	6	–		–	Hughes (1972)
Hoplias malabaricus	WB	240	3.16	–		–	Fernandes et al. (1994) Sakuragui et al. (2003)
Oncorhynchus mykiss	WB	240	6	–		–	Hughes (1972)
Tinca tinca	WB	250	3	–		–	Hughes (1972)
Amia calva	AB[b]	191	–	–		–	Crawford (1971)
Anabas testudineus	AB[a]	47.2	10	SBC	7.8	0.21	Hughes et al. (1973)
				LO	32.0	0.21	
Arapaima gigas	AB[a]	77	7.76	SB	–	–	Costa et al. (2007)
		78	9.61	SB	217.0	0.22	Present study
Channa punctatus	AB[b]	72	2.03	AS	39.2	0.78	Hughes and Munshi (1973) Hakim et al. (1978)
Clarias batrachus	AB[b]	83	7.67–12.4	SBC	15.5	–	Hughes and Munshi (1979)
				GF	3.4	–	Munshi (1985)
				AO	28.7	0.55	
Clarias mossambicus	AB[b]	22	2	SBC	10.2	0.31	Maina and Maloiy (1986)
				GF	–	–	
				AO	5.7	0.29	
Boleophthalmus boddarti	AB[b]	74	1.43	OC	6.4	1.22	Biswas et al. (1981)
		62	–		–	–	Low et al. (1990)
Heteropneustes fossilis	AB[b]	56	3.58	Sk	198.6	98.0	Hughes and Munshi (1973)
				AS	30.7	1.6	Hughes et al. (1974)
Lepidosiren paradoxa[c]	AB[a]	–	–	L	212.5	0.86	Hughes and Weibel (1976)
		0.38	80	L	523.7	1.56	Moraes et al. (2005)
				Sk	110.5	161.7	
Lepisosteus osseus	AB[b]	83	–	–		–	Crawford (1971)
Protopterus aethiopicus	AB[a]	–	–	L	1400	0.37	Maina and Maloiy (1985)
Pangasius hypophthalmus	AB[b]	–	–	SB	–	0.7	Podkowa and Goniakowska-Witalinska (1998)
Pterygoplichthys anisitsi	AB[b]	288	0.40	St	15.7	0.40–0.74	Cruz (2007) Cruz et al. (2009a,b)

WB, water breathing; AW, air breathing; AO, arborescent organ; AS, air sac; GF, gill fans; L, lungs; LO, labyrinth organ; OC, opercular chamber; SB, swim bladder; SBC, suprabranchial chamber; Sk, skin; St, stomach

[a] Obligated air-breathing fish.

[b] Facultative air-breathing fish.

[c] Body mass = 500 g (Hughes and Weibel, 1976) and Body mass = 620 ± 30 g (Moraes et al., 2005).

septum that stretches downwards between the body flanks, creating suction and filling the air-breathing organ (Farrell and Randall, 1978).

In conclusion, juvenile *A. gigas* needs to rise to the water surface to gulp air. Its gills surface, although similar to some facultative air-breathing fish, cannot function efficiently enough to fulfill all O_2 requirements. The lower morphometric D_{O_2} of the gills in addition to low oxygen solubility in the natural environment of *A. gigas* restricts O_2 uptake by the gills compared to swim bladder O_2 uptake from the air. Energy-requiring physiological mechanisms, however, result in greater CO_2 excretion through the gills despite a larger morphometric D_{CO_2} for the air-breathing organ.

Acknowledgments

The authors acknowledge the CAPES (Brazil) and DAAD (Germany) for financial support (Probral Program) to M.N. Fernandes and S.F. Perry and, FAPESP and CNPq to M.N. Fernandes. O.T.F. Costa and A.L. Cruz acknowledge CAPES and CNPq for their scholarships.

References

Banerjee, T.K., Mittal, A.K., 1976. Histochemistry and functional organisation of the skin of a 'live-fish' *Clarias batrachus* (Linn.) (Clariidae, Pisces). Mikroskopie 31, 333–349.

Bartels, H., 1971. Diffusion coefficients and Krogh's diffusion constants. In: Altman, P.L., Dittmer, P.S. (Eds.), Respiration and Circulation. Federation of American Societies for Experimental Biology, Bethesda, pp. 21–22.

Bicudo, J.E.P.W., Johansen, K., 1979. Respiratory gas exchange in the airbreathing fish, *Synbranchus marmoratus*. Environ. Biol. Fish 4, 55–64.

Biswas, N., Ojha, J., Munshi, J.S.D., 1981. Morphometrics of respiratory organs of an estuarine goby, *Boleophthalmus boddaerti*. Jpn. J. Ichthyol. 27, 316–326.

Brauner, C.J., Val, A.L., 1996. The interaction between O_2 and CO_2 exchange in the obligate air breather, *Arapaima gigas*, and the facultative air breather, *Lipossarcus pardalis*. In: Val, A.L., Almeida-Val, V.M.F., Randall, D.J. (Eds.), Physiology and Biochemistry of the Fishes of the Amazon. Instituto Nacional de Pesquisas da Amazônia, Manaus, pp. 101–110.

Brauner, C.J., Val, A.L., 2005. Oxygen transfer. In: Val, A.L., Almeida-Val, V.M.F., Randall, D.J. (Eds.), Fish Physiology. The Physiology of Tropical Fishes. Academic Press, New York, pp. 277–306.

Brauner, C.J., Matey, V., Wilson, J.M., Bernier, N.J., Val, A.L., 2004. Transition in organ function during the evolution of air-breathing; insights from *Arapaima gigas*, an obligate air-breathing teleost from the Amazon. J. Exp. Biol. 207, 1433–1438.

Carter, G.S., Beadle, L.C., 1931. The fauna of the swamps of the Paraguayan Chaco in relation to its environment. II: respiratory adaptations in the fishes. J. Linn. Soc. Lond. (Zool.) 37, 327–366.

Costa, O.T.F., Pedretti, A.C.E., Schmitz, A., Perry, S.F., Fernandes, M.N., 2007. Stereological estimation of surface area and barrier thickness of fish gills in vertical sections. J. Microsc. 225, 1–9.

Crawford, R.H., 1971. Aquatic and aerial respiration in the bowfin, longnose gar and Alaska blackfish. Ph.D. Thesis, University of Toronto, Toronto, Canada.

Cruz, A.L., 2007. O comportamento respiratório e a cascata de O_2 no cascudo de respiração bimodal *Pterygoplichthys anisitsi* Eigenmann e Kennedy, 1903 (Teleostei, Loricariidae). Ph.D. Thesis. Universidade Federal de São Carlos, São Carlos, Brazil.

Cruz, A.L., Fernandes, M.N., Perry, S.F., 2009a. Effect of histological processing and methacrylate sectioning on the area of gill tissue in teleost gill. Braz. J. Biol. 69, 631–637.

Cruz, A.L., Pedretti, A.C.E., Fernandes, M.N., 2009b. Stereological estimation of the surface area and oxygen diffusing capacity of the respiratory stomach of the air-breathing armored catfish fish *Pterygoplichthys anisitsi* (Teleostei: Loricariidae). J. Morphol. 270, 601–614.

Farrell, A.P., Randall, D.J., 1978. Air-breathing mechanics in two Amazonian teleosts, *Arapaima gigas* and *Hoplerythrinus unitaeniatus*. Can. J. Zool. 56, 939–945.

Fernandes, M.N., 1996. Morpho-functional adaptations of gills in tropical fish. In: Val, A.L., Almeida-Val, V.M.F., Randall, D.J. (Eds.), Physiology and Biochemistry of the Fishes of the Amazon. Instituto Nacional de Pesquisas da Amazônia, Manaus, pp. 181–190.

Fernandes, M.N., Rantin, F.T., Kalinin, A.L., Moron, S.E., 1994. Comparative study of gill dimensions of three erythrinid species in relation to their respiratory function. Can. J. Zool. 72, 160–165.

Fernandes, M.N., Moron, S.E., Sakuragui, M.M., 2007. Gill morphological adjustments to environment and the gas exchange function. In: Fernandes, M.N., Glass, M.L., Rantin, F.T., Kapoor, B.G. (Eds.), Fish Respiration and Environment. Science Publishers, Enfield, pp. 93–120.

Gee, J.H., Graham, J.B., 1978. Respiratory and hydrostatic functions of the intestine of the catfishes *Hoplosternum thoracatum* and *Brochis splendens* (Callichthyidae). J. Exp. Biol. 74, 1–16.

Gonzalez, R.J., Brauner, C.J., Wang, Y.W., Richards, J.G., Patrick, M.L., Xi, W., Matey, V., Val, A.L., 2010. Impact of ontogenetic changes in branchial morphology on gill function in *Arapaima gigas*. Physiol. Biochem. Zool. 83, 322–332.

Graham, J.B., 1997. Air-Breathing Fishes: Evolution, Diversity and Adaptation. Academic Press, New York.

Gundersen, H.J.G., Jensen, T.B., 1987. The efficiency of systematic sampling in stereology and its prediction. J. Microsc. 147, 229–263.

Gundersen, H.J.G., Bagger, P., Bendtsen, T.F., Evans, S.M., Korbo, L., Marcussen, N., Möller, A., Nielsen, K., Nyengaard, J.R., Pakkenberg, B., Sörensen, F.B., Vesterby, A., West, M.J., 1988. The new stereological tools: disector, fractionator, nucleator and point sampled intercepts and their use in pathological research and diagnosis. APMIS 96, 857–881.

Hakim, A., Munshi, J.S.D., Hughes, G.M., 1978. Morphometrics of the respiratory organs of the Indian green snakeheaded fish, *Channa punctata*. J. Zool. Lond. 184, 519–543.

Howard, C.V., Reed, M.G., 2007. Unbiased Stereology. Three-dimensional Measurement in Microscopy. Bios Scientific Publishers, Oxford.

Hughes, G.M., 1972. Morphometrics of fish gills. Resp. Physiol. 14, 1–25.

Hughes, G.M., Munshi, J.D.S., 1973. Nature of the air-breathing organs on the Indian fishes, *Channa*, *Amphipnous*, *Clarias* and *Saccobranchus* as shown by electron microscopy. J. Zool. Lond. 170, 245–270.

Hughes, G.M., Munshi, J.S.D., 1979. Fine structure of the gills of some Indian air-breathing fishes. J. Morphol. 160, 169–193.

Hughes, G.M., Weibel, E.R., 1976. Morphometry of fish lung. In: Hughes, G.M. (Ed.), Respiration of Amphibious Vertebrate. Academic Press, London, pp. 213–231.

Hughes, G.M., Dube, S.C., Munshi, J.S.D., 1973. Surface area of the respiratory organs of the climbing perch, *Anabas testudineus* (Pisces, Anabantidae). J. Zool. Lond. 170, 227–243.

Hughes, G.M., Singh, B.R., Guha, G., Dube, S.C., Munshi, J.S.D., 1974. Respiratory surface areas of an air-breathing siluroid fish, *Saccobranchus* (=*Heteropneustes*) *fossilis* in relation to body size. J. Zool. Lond. 172, 215–232.

Landolt, J.C., Hill, L.G., 1975. Observation of the gross structure and dimensions of the gills of three species of gars (Lepisosteidae). Copeia 1975, 470–475.

Low, W.P., Ip, Y.K., Lane, D.J.W., 1990. A comparative study of the gill morphometry in the mudskippers – *Periophthalmus chrysospilos*, *Boleophthalmus boddaerti* and *Periophthalmodon schlosseri*. Zool. Sci. 7, 29–38.

Maina, J.N., Maloiy, G.M.O., 1985. The morphometry of the lung of the African lungfish (*Protopterus aethiopicus*): its structural functional correlations. Proc. Roy. Soc. Lond. Biol. Sci. 224, 399–420.

Maina, J.N., Maloiy, G.M.O., 1986. The morphology of the respiratory organs of the African air-breathing catfish (*Clarias mossambicus*): a light, electron and scanning microscopic study, with morphometric observations. J. Zool. Lond. 209, 421–445.

Maina, J.N., King, A.S., Settle, G., 1989. An allometric study of pulmonary morphometric parameters in birds, with mammalian comparisons. In: Bone, Q. (Ed.), Biological Sciences. Royal Society, London, pp. 1–57.

Mazon, A.F., Fernandes, M.N., Nolasco, M.A., Severi, W., 1998. Functional respiratory gill area of two active rheophilic teleosts, *Plagioscion squamosissimus* and *Prochilodus scrofa*. J. Fish Biol. 52, 50–61.

Michel, R.P., Cruz-Orive, L.M., 1988. Application of the Cavalieri principle and vertical sections method to lung: estimation of volume and pleural surface area. J. Microsc. 150, 117–136.

Moraes, M.F.P.G., Höller, S., Costa, O.T.F., Glass, M.L., Fernandes, M.N., Perry, S.F., 2005. Morphometric comparison of the respiratory organs in the South American lungfish *Lepidosiren paradoxa* (Dipnoi). Physiol. Biochem. Zool. 78, 546–559.

Munshi, J.S.D., 1985. The structure, function and evolution of the accessory respiratory organs of air-breathing fishes of India. Fortschr. Zool. 30, 353–366.

Pereira-Filho, M., Cavero, B.A.S., Roubach, R., Ituassu, D.R., Gandra, A.L., Crescêncio, R., 2003. Cultivo do pirarucu (*Arapaima gigas*) em viveiro escavado. Acta Amazonica 33, 715–718.

Perna, S.A., Fernandes, M.N., 1996. Gill morphometry of the facultative air-breathing loricariid fish, *Hypostomus plecostomus* (Walbaum) with special emphasis to aquatic respiration. Fish Physiol. Biochem. 15, 213–220.

Perry, S.F., 1978. Quantitative anatomy of the lungs of the red-eared turtle, *Pseudemys scripa elegans*. Respir. Physiol. 35, 245–262.

Perry, S.F., 1983. Reptilian lungs. Functional anatomy and evolution. Adv. Anat. Embryol. Cell Biol. 70, 1–81.

Perry, S.F., Hein, J., Dieken, E.V., 1994. Gas exchanges morphometry of the lungs of the tokay, *Gekko gecko* L. J. Comp. Physiol. B 164, 196–206.

Podkowa, D., Goniakowska-Witalinska, L., 1998. The structure of the airbladder of the catfish *Pangasius hypophthalmus* Roberts and Vidthayanon 1991, (previously *P. sutchi* Fowler 1937). Folia Biol. 46, 189–196.

Powell, F.L., 1989. Lung structure and function. Birds. In: Wood, S.C. (Ed.), Comparative Pulmonary Physiology. current Concepts. Marcel Dekker Inc., New York, 00 pp. 237–255.

Ramos, C.A., 2008. Caracterização morfológica e morfométrica dos parâmetros branquiais de *Arapaima gigas*, durante o desenvolvimento. Ms thesis. Universidade Federal de São Carlos, pp.77.

Randall, D.J., Farrell, A.P., Haswell, M.S., 1978. Carbon dioxide excretion in the pirarucu (*Arapaima gigas*), an obligate air-breathing fish. Can. J. Zool. 56, 977–982.

Sakuragui, M.M., Sanches, J.R., Fernandes, M.N., 2003. Gill chloride cell proliferation and respiratory responses to hypoxia of the neotropical erythrinid fish *Hoplias malabaricus*. J. Comp. Physiol. B 173, 309–317.

Santos, C.T.C., Fernandes, M.N., Severi, W., 1994. Respiratory gill surface area of a facultative air-breathing loricariid fish, *Rhinelepis strigosa*. Can. J. Zool. 72, 2009–2013.

Sawaya, P., 1946. Sobre a biologia de alguns peixes de respiração aérea (*Lepidosiren paradoxa* Fitzinger e *Arapaima gigas* Cuvier). Biol. Fac. Univ. São Paulo (Zool.) 11, 255–285.

Silva, J.M., Hernandez-Blazquez, F.J., Julio Jr., H.F., 1997. A new accesory respiratory organ in fishes: morphology of the respiratory purses of *Loricariichthys platymetopon* (Pisces, Loricariidae). Ann. Sci. Nat. Zool. 18, 93–103.

Sollid, J., Nilsson, G.E., 2006. Plasticity of respiratory structures—adaptive remodeling of fish gills induced by ambient oxygen and temperature. Resp. Physiol. Neurobiol. 154, 241–251.

Sollid, J., De Angelis, P., Gundersen, K., Nilsson, G.E., 2003. Hypoxia induces adaptive and reversible gross morphological changes in crucian carp gills. J. Exp. Biol. 206, 3667–3673.

Stevens, E.D., Holeton, G.F., 1978. The partitioning of oxygen uptake from air and from water by the large obligate air-breathing teleost pirarucu (*Arapaima gigas*). Can. J. Zool. 56, 974–976.

Val, A.L., Almeida-Val, V.M.F., 1995. Fishes of the Amazon and Their Environment – Physiological and Biochemical Aspects. Zoophysiology Series, vol. 32. Springer-Verlag, Berlin, 224 p.

Watson, R.R., Fu, Z., West, J.B., 2007. Morphometry of the extremely thin pulmonary blood–gas barrier in the chicken lung. Am. J. Physiol. Lung Cell. Mol. Physiol. 292, L677–L769.

Weibel, E.R., Knight, B.W., 1964. A morphometric study on the thickness of the pulmonary air–blood barrier. J. Cell Biol. 21, 367–384.

West, J.B., Watson, R.R., Fu, Z., 2006. The honeycomb-like structure of the bird lung allows a uniquely thin blood-gas barrier. Respir. Physiol. Neurobiol. 152, 115–118.